IV International Conference on Computational Methods for Coupled Problems in Science and Engineering
COUPLED PROBLEMS 2011
M. Papadrakakis, E. Oñate and B. Schrefler (Eds)

HYDROMECHANICAL ANALYSIS IN GEOTECHNICAL ENGINEERING USING THE MATERIAL POINT METHOD

F. ZABALA[*] AND E. ALONSO[**]

[*] Instituto de Investigaciones Antisísmicas- Universidad Nacional de San Juan
Av. Libertador San Martín Oeste 1290, 5400, San Juan, Argentina
E-mail: fzabala@unsj.edu.ar

[**] Departamento de Ingeniería del Terreno, Cartográfica y Geofísica
Universidad Politécnica de Cataluña- Edificio D2, Campus Norte UPC
Gran Capitán s/n, 08034 Barcelona, Spain
Email: eduardo.alonso@upc.edu

Key words: Material Point Method, pore pressure, finite strain.

Abstract. The explicit version of the Material Point Method [1] has been extended in order to model coupled hydromechanical saturated problems. MPM discretizes the continuum, which is considered as a saturated soil-fluid mixture, by dividing it into particles or material points. The discrete movement equations are not solved at the material points. Instead a support mesh, built to cover the domain of the problem, is used. In this paper it is assumed that particles carry all the variables needed to represent the state of the continuum including the pore pressure as a variable associated with each particle. The particle pore pressure increment is calculated explicitly using the equation of fluid mass balance, from the particle volumetric deformation and the fluid velocity relative to the soil skeleton, at the particle location.
The shape functions used for the mesh elements are usually the same bi-linear functions of the Finite Element Method and therefore the background mesh elements suffer the same drawbacks. These drawbacks include: volumetric locking for quasi-incompressible materials when four particles per cell are used, which is equivalent to four integration points in the finite element method, pressure instability for quasi-incompressible and low permeability materials and the generation of zero energy modes when one particle per cell is used, which corresponds to reduced integration in the finite element method. The MPM original version has also the disadvantage of generating "noise" in the solution [2] when a particle pass from one cell to another. A simple procedure that can be used to reduce instabilities is to consider constant stress at each cell equal to the stress average of the particles which are in the cell at the instant k. In this case the internal forces are obtained in the same way as in the finite element method when one point of integration is used, using the gradient of the shape functions calculated in the cell center. In this work, to avoid volumetric locking and simultaneously achieve a stable behavior, internal forces and pressure increments at the nodes are calculated using the gradients calculated at the cell center.

The procedure is completely explicit and has proved to be stable for the low permeability values used to model the foundation of Aznalcollar dam. The simulation of Aznalcollar dam progressive failure is presented as an example [3].

1 INTRODUCTION

The method was initially described by Sulsky et al. [1] and by Sulsky and Schreyer [5]. The Material Point Method discretizes the continuum dividing it into particles. A mass is assigned to each particle which remains fixed during all the calculation process, thus assuring mass conservation. Other initial values, such as velocities, strains and stresses, are also assigned to the material points. The discrete movement equations are not solved at the material points. Instead a support mesh, built to cover the domain of the problem, is used. This mesh is composed by elements of the same type as those used in finite element method. For simplicity, it is common to use four nodes bi-linear quadrilateral elements. The boundary conditions are imposed at the mesh nodes and the movement equations are incrementally solved. Then the quantities carried by the material points are updated through the interpolation of the mesh results, using the same shape functions. The information associated with the mesh is not necessary in the following step of the analysis; therefore it can be discarded, taking care of preserving the boundary conditions that may have been established. It is possible to discretize the momentum conservation equation through the application of standard Galerkin weighted residual method ([1], [5]). The derived mass matrix varies in time, and must be calculated for each step of the analysis. To reduce the computational cost of the procedure, a diagonal mass matrix can be used; therefore the movement equations are decoupled, and can be written for a node and for the k time step as:

$$m_i^k \mathbf{a}_i^k = \mathbf{f}_i^{\text{int},k} + \mathbf{f}_i^{\text{ext},k} \qquad (1)$$

where $\mathbf{f}_i^{\text{int}}$ and $\mathbf{f}_i^{\text{ext}}$ are the vectors of internal and external forces at the node i, respectively, m_i is the mass of node i and a_i is the node acceleration.

2 MPM COUPLED HYDRO-MECHANICAL ANALYSIS

MPM is very well suited for dealing with finite strains and large displacements that are developed when collapse or near collapse problems are studied. In order to model coupled hydro-mechanical saturated problems the continuum can be considered as a saturated soil-fluid mixture. In this paper it is assumed that particles carry all the variables needed to represent the state of the continuum including the pore pressure as an associated variable.

The formulation of the equations which describe the behavior of a saturated porous medium was first developed by Biot [4] and then extended by Zienkiewicz and others [6], [7]. The governing equations can be simplified if the fluid acceleration relative to the soil skeleton is small as follows.

The balance of momentum is written for the mixture as:

$$\nabla \cdot \boldsymbol{\sigma} + \rho \mathbf{b} = \rho \mathbf{a} \qquad (2)$$

$\boldsymbol{\sigma}$ is the total stress tensor, $\mathbf{b}$ are the body forces, $\mathbf{a}$ is the acceleration and ρ is the density of the mixture,

$$\rho = (1\text{-}n)\,\rho_s + n\,\rho_f \qquad (3)$$

n is the porosity, ρ_s is the solid density and ρ_f is the fluid density.

The balance of fluid mass is written,

$$\dot{\varepsilon}_v + \nabla \cdot \mathbf{w} + \frac{\dot{p}}{Q} = 0 \qquad (4)$$

$\mathbf{w}$ is the Darcy velocity, $\nabla \cdot \mathbf{w}$ the divergence of velocity, $\dot{\varepsilon}_v$ is the volumetric strain variation of soil skeleton and $\dot{p}$ the fluid pressure variation. Q is the combined compressibility modulus of the fluid and solid phase.

$$\frac{n}{K_f} + (1-n)\frac{1}{K_s} = 1/Q \qquad (5)$$

K_f is the fluid bulk modulus, K_s is the bulk modulus of the grains material.

The Darcy equation is written:

$$\mathbf{w} = -\frac{\mathbf{k}}{\gamma_f}\left[\nabla p - \rho_f\,\mathbf{b} + \rho_f\,\mathbf{a}\right] \qquad (6)$$

Where $\mathbf{k}$ is the permeability tensor, γ_f the specific weight of fluid and ∇p the pressure gradient.

The relationship between effective stress and total stress is:

$$\boldsymbol{\sigma} = \boldsymbol{\sigma}' - \alpha p\,\mathbf{m} \qquad (7)$$

$\boldsymbol{\sigma}'$ is the effective stress, p the pore pressure (positive for compression), $m_{ij} = \delta_{ij}$,

δ_{ij}: Kronecker Delta, $\alpha = 1 - \frac{K_t}{K_s}$ and K_t is the bulk modulus of soil skeleton.

For soils $K_t << K_s$ and $\alpha \cong 1$

These equations together with boundary conditions can be discretized and solved numerically using as unknowns the displacements and the pore pressure.

2.1 MPM discretization of the equations related to the fluid.

The pore pressure increment in a particle is calculated explicitly using the equation of fluid mass balance, from the particle volumetric deformation and the fluid velocity relative to the soil skeleton, at the particle location.

From Equation(4):

$$\Delta p + Q(\dot{\varepsilon}_v + \nabla \cdot \mathbf{w})\Delta t = \Delta p + Q(\Delta \varepsilon_v + \nabla \cdot \mathbf{w}\Delta t) = 0 \qquad (8)$$

$\Delta\varepsilon_v$ is the volumetric strain increment at a point in the continuum and Δp the pore pressure increment at the end of time interval Δt.

The boundary conditions imposed on the mesh are:

$$\text{in } \Gamma_p : p - \overline{p} = 0$$
$$\overline{p} : \text{Pressure imposed on the boundary } \Gamma_p \quad (9)$$

$$\text{in } \Gamma_w : k\frac{\partial p}{\partial n} - \overline{w} = w_n - \overline{w} = 0$$
$$\overline{w} : \text{Fluid velocity enforced in } \Gamma_w \quad (10)$$
$$w_n : \text{velocity normal to boundary } \Gamma_w$$

The standard Galerkin method is applied to Equation (8) using weighting functions for the pressures equal to those used for the interpolation of displacements.

$$\int_{\Omega_t} N_i \, [\Delta p + Q(\Delta\varepsilon_v + \nabla \cdot \mathbf{w}\Delta t)] \, \mathrm{d}\Omega \; - \int_{\Gamma_w} N_i \, (w_n - \overline{w})\Delta t \, \mathrm{d}\Gamma = 0 \quad (11)$$

N_i is the shape function for node i.
Integrating by parts,

$$\int_{\Omega_t} N_i \, \nabla \cdot \mathbf{w}\Delta t \, \mathrm{d}\Omega \; = \int_{\Gamma_t} N_i \mathbf{w} \cdot \mathbf{n}\Delta t \mathrm{d}\Gamma \; - \int_{\Omega_t} \nabla N_i \cdot \mathbf{w}\Delta t \, \mathrm{d}\Omega \quad (12)$$

results in:

$$\int_{\Omega_t} N_i \, \Delta p \, \mathrm{d}\Omega + \int_{\Omega_t} N_i \, Q \, \Delta\varepsilon_v \mathrm{d}\Omega - \int_{\Omega_t} \nabla N_i \cdot \mathbf{w}\Delta t \, \mathrm{d}\Omega \; + \int_{\Gamma_w} N_i \overline{w}\Delta t \mathrm{d}\Gamma = 0 \quad (13)$$

The particle pressure increment is approximated using the pressure increments at the nodes using the same interpolation functions used for displacements:

$$\Delta p_p^k = \sum_{j=1}^{N_n} \Delta p_j^k N_j \left(\mathbf{x}_p^k \right) \quad (14)$$

Δp_i^k is the node pressure increment at time k , Δp_p^k the particle pressure increment at time k and $\mathbf{x}_p^k$ is the particle position.

Replacing the integrals in equation 13 by sums of quantities at the material points, the mesh nodes pressure increments at time *k* can be computed. In these integrals the material points or particles correspond to the integration points in the finite element method. The first of the integrals of equation 13 is equal to:

$$\int_{\Omega_t} N_i \ \Delta p \ \mathrm{d}\Omega = \sum_{p=1}^{N_p} N_i\left(\mathbf{x}_p^k\right) \Delta p_p^k \ V_p = \sum_{p=1}^{N_p} N_i\left(\mathbf{x}_p^k\right) \sum_{j=1}^{N_n} \Delta p_j^k \ N_j\left(\mathbf{x}_p^k\right) V_p$$
$$\sum_{j=1}^{N_n} \Delta p_j^k \ \sum_{p=1}^{N_p} N_i\left(\mathbf{x}_p^k\right) N_j\left(\mathbf{x}_p^k\right) V_p = \sum_{j=1}^{N_n} \Delta p_j^k V_{ij}^k \qquad (15)$$

Where V_p is the particle volume. The element volume matrix V_{ij} can be lumped at the nodes to give a diagonal matrix V_i:

$$V_{ij}^k = \sum_{p=1}^{N_p} N_i\left(\mathbf{x}_p^k\right) N_j\left(\mathbf{x}_p^k\right) V_p \qquad (16)$$

$$V_i^k = \sum_{p=1}^{N_p} N_i\left(\mathbf{x}_p^k\right) V_p \qquad (17)$$

$$\sum_{p=1}^{N_p} N_i\left(\mathbf{x}_p^k\right) \Delta p_p^k \ V_p = \sum_{j=1}^{N_n} \Delta p_j^k \ V_{ij} \cong \Delta p_i^k \ V_i^k \qquad (18)$$

Thus the pressure increments at the nodes can be calculated explicitly:

$$\Delta p_i^{k+1} = \frac{1}{V_i} Q \left[\sum_{p=1}^{N_p} \left(N_i(\mathbf{x}_p^k) \ \Delta \varepsilon_{v_p}^k - \nabla N_i(\mathbf{x}_p^k) \cdot \mathbf{w}_p^k \Delta t \right) V_p + \int_{\Gamma_q} N_{\mathrm{i}} \ \bar{w} \ \Delta t \ \mathrm{d}\Gamma \right] \qquad (19)$$

The Darcy equation is used to calculate the flow velocities at each particle:

$$\mathbf{w}_p^k = -\frac{\mathbf{k}}{\gamma_f} \left[\nabla p(\mathbf{x}_p^k) - \rho_f \ \mathbf{b} + \rho_f \ \mathbf{a}_p^k \right] \qquad (20)$$

The pressure gradient is evaluated using the field interpolated from the node's pressures at the k instant. This pressure field can be approximated in the same way as the pressure increment:

$$p_p^k = \sum_{j=1}^{N_n} p_j^k N_j\left(\mathbf{x}_p^k\right) \qquad (21)$$

where p_i^k is the node i pressure for instant k and p_p^k the particle pressure at instant k. Then,

$$\sum_{p=1}^{N_p} N_i\left(\mathbf{x}_p^k\right) p_p^k V_p = \sum_{j=1}^{N_n} p_j^k V_{ij} \cong p_i^k V_i \qquad (22)$$

$$p_i^k = \frac{1}{V_i} \sum_{p=1}^{Np} N_i\left(\mathbf{x}_p^k\right) p_p^k \ V_p \qquad (23)$$

Thus the pressure gradient can be calculated with the expression:

$$\nabla p(\mathbf{x}_p^k) = \sum_{i=1}^{N_n} p_i^k \nabla N_i\left(\mathbf{x}_p^k\right) \qquad (24)$$

Finally the following equation is used to update the particle pressures:

$$p_p^{k+1} = p_p^k + \sum_{i=1}^{N_n} \Delta p_i^{k+1} N_i\left(\mathbf{x}_p^k\right) \qquad (25)$$

The nodal pressures are calculated with equation (23) using the pressures carried by the material points which were obtained in the previous step of the solution. This calculation scheme is similar to the procedure used in MPM to obtain the momentum at the mesh nodes. The pressure gradient is obtained through equation (24) from the mesh pressure field. The fluid flow relative velocity, at the coordinates of particles, is calculated using the Darcy equation(20). The pressure increment at the nodes is calculated using equation(19). The terms in this equation: volumetric strain increment, velocity divergence and external flow are accumulated at the nodes by adding the contribution of the particles. Boundary conditions are imposed on the mesh. The particles pressures are updated through equation (25) for use in the next step. At the end of the time interval the pressures at the nodes are not useful and can be discarded because the particles carry the information on pore pressures.

2.2 Stability of the solution

The shape functions used for the mesh elements are typically the same bi-linear functions used in the finite element method and therefore the background mesh elements suffer the same drawbacks. These drawbacks include: volumetric locking for quasi-incompressible materials when four particles per cell are used, which is equivalent to four integration points in the finite element method; pressure instability for quasi-incompressible and low permeability materials and the generation of zero energy modes when one particle per cell is used, which corresponds to reduced integration in the finite element method.

Mixed displacement-pressure approximations are known to suffer pressure instability if the Babuska-Brezzi condition is not fulfilled. In the framework of the finite element method an element is stable without using special procedures if the number of degrees of freedom used to interpolate the pressure is lower than the number used to interpolate the displacements.

The same shape functions are used in 2.1 to interpolate displacements and pressures in the discretization of the equations for the fluid. Therefore, pressure instability is expected for this formulation.

MPM original version has also the disadvantage of generating "noise" in the solution [2] when a particle pass from one cell to another. This noise is due to the discontinuity of the interpolation function gradient which is involved in the calculation of internal forces [2]. A simple procedure that can be used to reduce this type of instability is to consider a constant stress at each cell equal to the stress average of the particles which are in the cell at the instant *k*. In this case the internal forces are obtained in the same way as in the finite element method when one point of integration is used, using the gradient of the shape functions calculated in the cell center. When there are more or less particles in a cell than the original amount of

particles per cell, the average density of the cell increases or decreases artificially and hence the internal forces due to the contribution of that cell can be approximated as follows:

$$\mathbf{f}_{i-cell}^{\text{int},k} = -\sum_{p=1}^{N_{p-cell}^{k}} m_p \mathbf{G}_{ip}^{k} \mathbf{S}_{p}^{k} = -\sum_{p=1}^{N_{p-cell}^{k}} m_p \mathbf{G}_{ip}^{k} \frac{\boldsymbol{\sigma}_{p}^{k}}{\rho^{k}_{cell}} = \sum_{p=1}^{N_{p-cell}} \mathbf{G}_{ip}^{k} \boldsymbol{\sigma}_{p}^{k} \frac{V_{cell}}{N_{p-cell}^{k}} = \mathbf{G}_{i0} \sum_{p=1}^{N_{p-cell}} \boldsymbol{\sigma}_{p}^{k} \frac{V_{cell}}{N_{p-cell}^{k}} \qquad (26)$$

$$\rho^{k}_{cell} = \frac{N_{p-cell}^{k} m_p}{V_{cell}}$$

where :

m_p : particle mass

$\mathbf{G}_{ip}^{k} = \nabla N_i(\mathbf{x})\big|_{\mathbf{x}=\mathbf{x}_p^k}$: shape function gradient at particle location

$\mathbf{G}_{i0}$: shape function gradient at cell center

$\mathbf{S}_{p}^{k} = \frac{\boldsymbol{\sigma}_{p}^{k}}{\rho^{k}}$:specific stress

ρ^{k}_{cell} : average cell density at step *k*

N_{p-cell}^{k} *:* number of particles in the cell at step *k*

V_{cell} :cell volume (constant)

In equation (26) the gradients at particles positions are approximated by the gradient at the center of the element and this is equivalent to the procedure of averaging the stresses of the particles which are in a cell. On the other hand the pressure instability is avoided by imposing a constant pressure increment to the particles in a cell equal to the pressure increment calculated at the element center instead of calculating the pressure increment at positions of the particles (Equation 25).

Figure 1 shows a rigid footing resting on a water-saturated porous material with zero permeability. This problem was solved with 4 particles per cell. The average stress of the particles in the cell and the gradient calculated at the center of the element were used for compute internal forces. Also the particles pressure increment is calculated at the center of the element. A constant vertical velocity was imposed to the particles of the footing. Figure 2.a shows an instant pore pressure distribution for an elastic material and Figure 2.b the same for a Mohr-Coulomb elastic-plastic material with cohesion and friction. The procedure is stable and there are not pressure oscillations. Figure 3 shows contours of equivalent plastic strain for the Mohr-Coulomb material. If the internal forces are calculated using the gradients in the positions of the particles, we obtain the classical pressure instability shown in Figure 4.

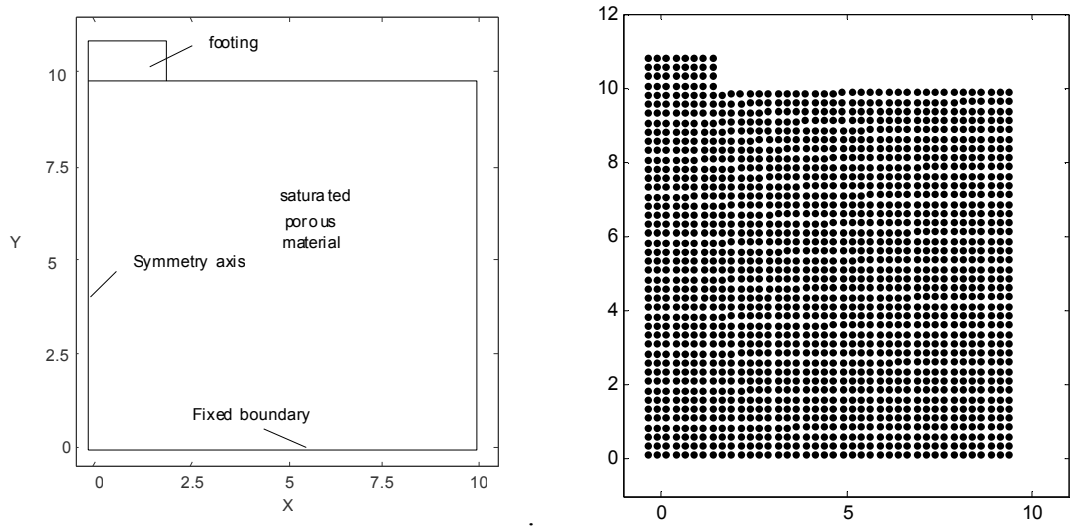

Figure 1. Rigid footing resting on saturated porous material.

a) Geometry b) Particle model.

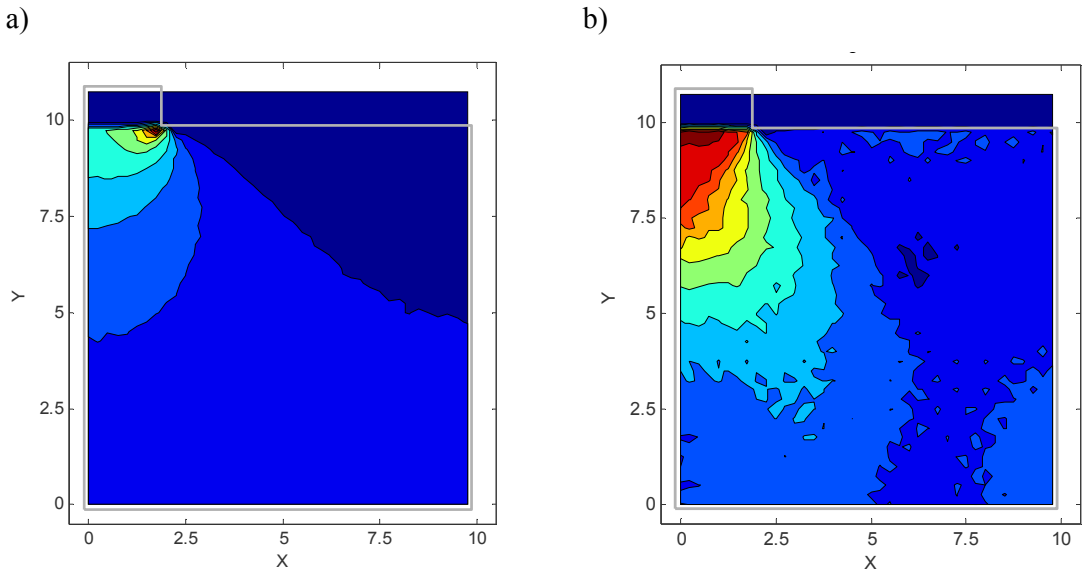

Figure 2. Rigid footing. Pore pressure contours for zero permeability

a) Elastic material b) Mohr Coulomb material.

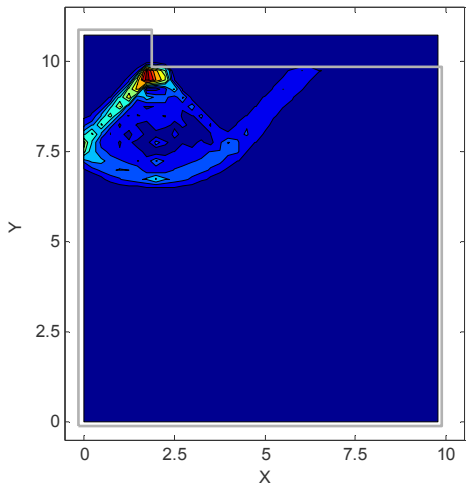

Figure 3. Equivalent plastic shear strain for Mohr Coulomb material

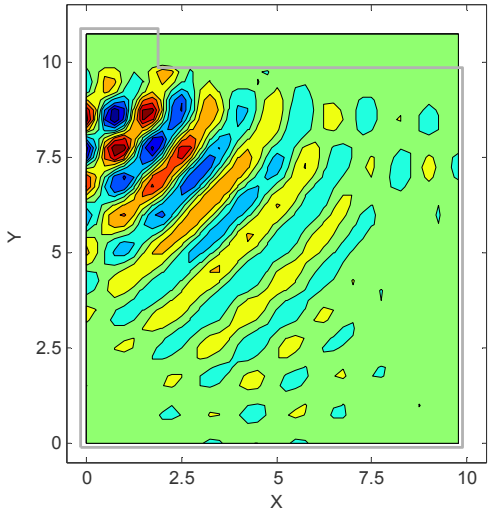

Figure 4. Pressure instability

2.3 Impulsive load applied to a soil column.

This section compares MPM results for a soil column (Figure 5.a) with those obtained by Mira et al. [8] with Q8P4 finite elements (elements with 8 displacement and 4 pressure degrees of freedom) in order to check the stability of the calculation algorithm. Figure 5.b compares results for pressure distribution one second after the application of an impulsive load. Pressure instability occurs if pressure increments at positions of the particles are used for updating the particle pressures.

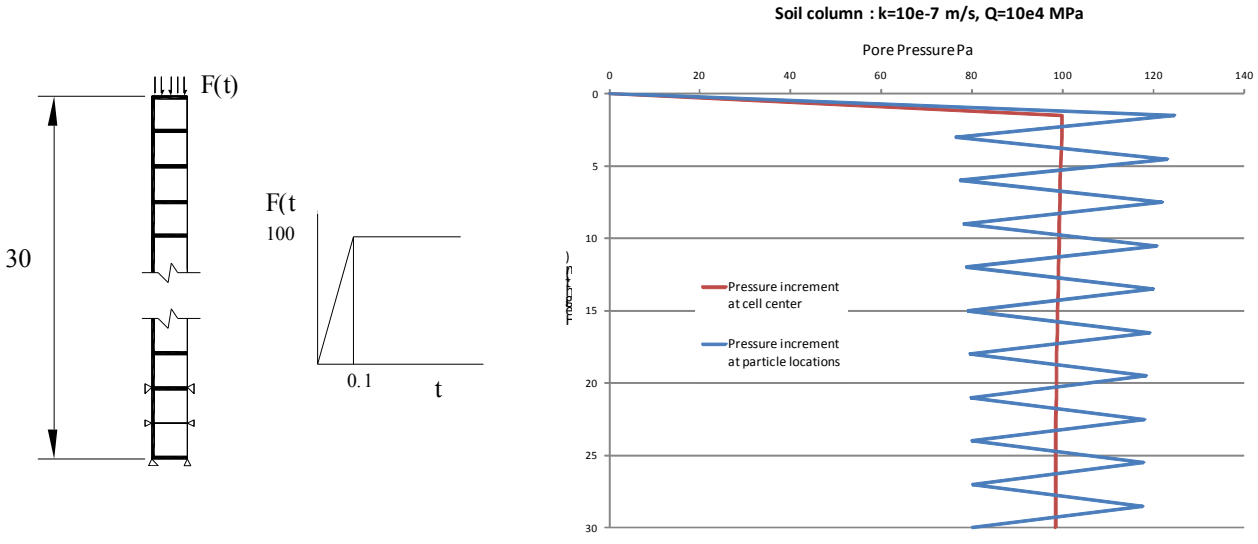

Figure 5. a) Soil column under impulsive load. b) Pore pressure distribution.

3 MODELLING AZNALCOLLAR DAM FAILURE

MPM in its explicit version, including the hydro-mechanical coupling for a water-saturated material, has been used for modeling Aznalcollar dam failure ([9], [10], [3]). It is believed that this dam failed progressively due the fragility of the very low permeability foundation clay, in which high pore pressures persisted during twenty years of construction until failure, and the downstream method of construction which generate high shear stresses under the downstream slope. The dam failed and moved forward as a solid body in the way indicated in Figure 6. The failure was explained by the development of a continuous subhorizontal failure surface located 14 m under the contact between the dam and its foundation at the dam axis.

The construction and filling of the reservoir was simulated in stages (Figure 9). Figure 8 shows the vertical pore pressures distribution for the foundation clay in a zone of the tailings pond, away from the dam, for the 9, 13 and 15 stages of construction. The pressures calculated with MPM are compared with Terzaghi's solution. Also a point is plot, for stage 15, which represents the pressure measured at the approximate depth of the sliding surface in a not failed section located north to the failure zone. A boundary condition of hydrostatic pressure was applied at the bottom of the modeled foundation layer, which is considered fixed during construction. This hypothesis is based on field data from the aquifer that lies under the clay layer. A deep piezometer installed in the sand under the clay measured pore pressure equivalent to the height of the clay layer. The top boundary condition is variable and equal to the height of the tailings, which were always kept under water for each stage. A free water condition was considered in the upper layer of downstream alluvium.

Figure 8 shows contours of equivalent plastic shear strain for different stages of construction. The development of localization bands within the clay foundation and the tailings deposit are shown. The concentration of plastic shearing strains started underneath the downstream slope of the rockfill dam. The shearing band extended first downstream and then in the upstream direction. The shearing band defines a horizontal failure surface that eventually bends upwards below the upstream toe of the dam slope and crosses the tailings' deposit.

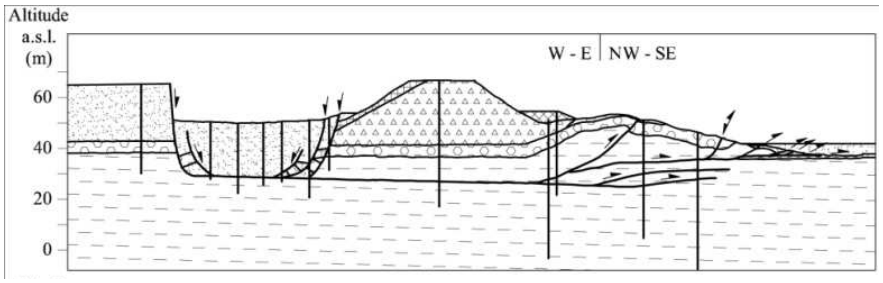

Figure 6. Cross-section of slide. Geometry after the slide, as interpreted from borehole data and surface topography [9]

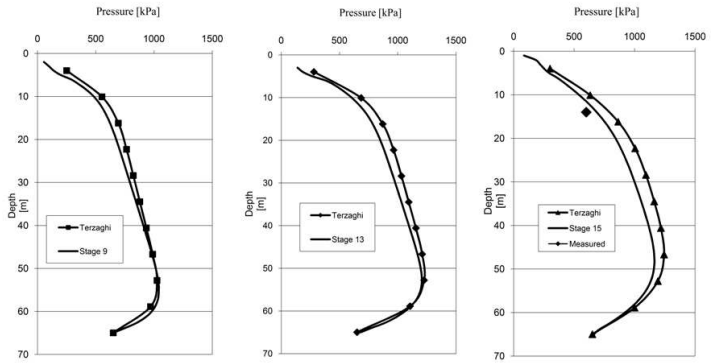

Figure 7. Pore pressure distribution at foundation.

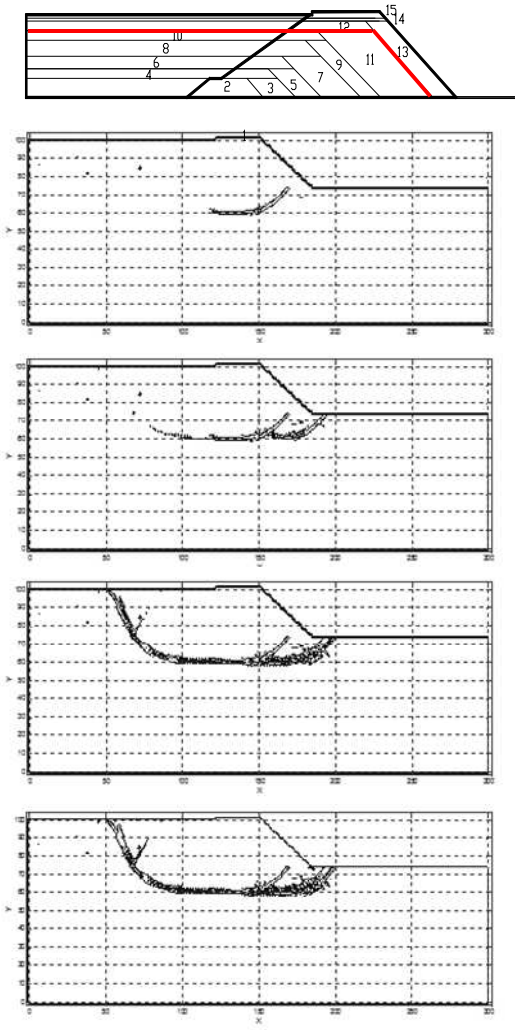

Figure 8. Sequence of contours of equal equivalent plastic strain, 1% and 5%. cv = 0.001 cm2/seg, $K_0 = 1$

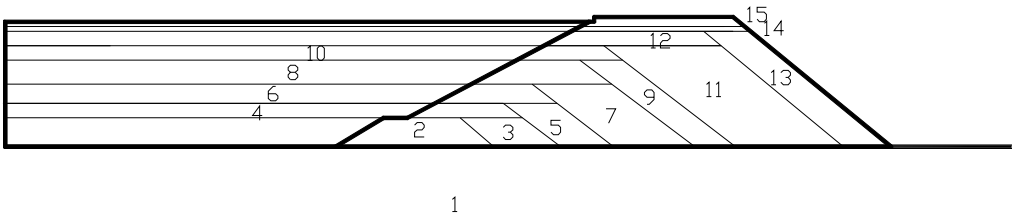

Figure 9. Geometry of the model and construction sequence of the dam

4 CONCLUSIONS

The Material Point Method was extended to model hydro-mechanical geotechnical problems. Pressure instability is circumvented using concepts of the Finite Element Method. A relative large scale problem of dam construction and failure was successfully solved with the procedure shown in this paper.

REFERENCES

[1] Sulsky, D., Z. Chen, & H. L. Schreyer. A Particle Method for History-Dependent Materials. Computer Methods in Applied Mechanics and Engineering. Vol. 118(1), pp 179-96. (1994).

[2] Bardenhagen, S. G. & E. M. Kober. The Generalized Interpolation Material Point Method.Computer Modeling in Engineering & Sciences. Vol.5(6), 477-95.(2004).

[3] Zabala, F & Alonso, E. E.. Progressive failure simulation of Aznalcollar dam using the Material Point Method. Géotechnique, doi: 10.1680/geot. (2011)

[4] Biot M. A..General theory of three dimensional consolidation. J. Appl. Phys. 12, 155-164. (1941)

[5] Sulsky, D. & H. L. Schreyer. Axisymmetric Form of the Material Point Method with Applications to Upsetting and Taylor Impact Problems. Computer Methods in Applied Mechanics and Engineering. 139(1), 409-29. (1996).

[6] Zienkiewicz O.C., Chang C.T. & Bettess P.. Drained,undrained, consolidating and dynamic behavior assumptions in soils. Geotechnique 30, No. 4, 385–395. (1980)

[7] Zienkiewicz O.C., Shiomi T..Dynamic behavior of saturated porous media: the generalized Biot formulation and its numerical solution, Int. J. Numer. Anal. Methods Geo-mech. 8, 71–96. (1984).

[8] Mira P., Pastor M., Li T., Liu X.. A New Stabilized Enhanced Strain Element with Equal Order of Interpolation for Soil Consolidation Problems. Computer Methods in Applied Mechanics and Engineering. 192(37), pp 4257-4277.(2003)

[9] Alonso, E. E. & Gens, A. (2006a). Aznalcóllar dam failure. Part 1: Field observations and material properties Geotechnique, 56, No. 3, 165–183

[10] Gens A. & Alonso E. E. (2006). Aznalcollar Dam Failure. Part 2: Stability Conditions and Failure Mechanism. Géotechnique. 56 No.3, pp 185-201.